Applying different types of artificial neural network for modeling thermal conductivity of nanofluids containing silica particles

Akbar Maleki[1] · Arman Haghighi[2] · Misagh Irandoost Shahrestani[3] · Zahra Abdelmalek[4,5]

Abstract

Nanofluids are widely applicable in thermal devices with porous structures. Silica nanoparticles have been dispersed in different heat transfer fluids in order to increase their thermal conductivity and heat transfer capability. In this study, group method of data handling (GMDH) and multilayer perceptron artificial neural networks are applied for determining thermal conductivity of nanofluids with silica particles and different base fluids such as ethylene glycol, glycerol, water and ethylene glycol–water mixture. For cases with multilayer perceptron models, trained by applying scaled conjugate gradient (SCG) and Levenberg–Marquardt (LM) have been tested as two different training algorithms. The outputs of the applied models have good agreement with the values obtained in experimental studies. The values of R^2 in the optimum conditions of using GMDH, LM and SCG are 0.9997, 0.9991 and 0.9998, respectively. In addition, the MSE values of the mentioned methods are approximately 0.000010, 0.000032 and 0.0000078, respectively.

Introduction

The need to improve the efficiency of engineering systems in various sectors such as chemical, mechanical, electronic and marine industries is rapidly increasing. There has been a great deal of research in these fields over the past years published as journal or conference papers [1–4]. These research spans from investigations studying heat transfer rate in human body [5, 6] to those looking for ways of increasing heat transfer coefficient in heat exchangers and industrial heat recovery steam generators [7–10] and fuel cells [11]. The use of nanofluids which are mixtures of a basic fluid with metallic or non-metallic solid particles at nanoscale has attracted the attention of many scientists during these years [12]. For instance, Choi [13] introduced the use of nanoparticles with base fluids to tackle the problem of low thermal conductivity of fluids. In this investigation, the need for more energy-efficient techniques was addressed by using copper nanoparticles. The results revealed considerable reduction in pumping power in heat exchangers. Thereafter, much research has been done that emphasizes the importance of using nanofluids to improve thermal performance of systems. Nanofluids are able to modify heat transfer of devices with various dimensions [14, 15]. Some studies focused on the use of nanofluids in conventional channels with macroscale dimensions [16–18] while others studied utilization of nanofluids in microchannels [19–22]. The effect of different nanoparticles types and various base fluids was studied as well [23–25].

It is important to know the thermophysical properties of nanofluids in order to model their heat transfer in different types of mediums such as porous or conventional [26–31]. Thus, a lot of research has focused on prediction of thermal conductivity of nanofluids. In a review article by Ahmadi et al. [32], it was shown that an increase in concentration

✉ Akbar Maleki
akbar.maleki20@yahoo.com; a_maleki@shahroodut.ac.ir

✉ Zahra Abdelmalek
zahraabdelmalek@duytan.edu.vn

1 Faculty of Mechanical Engineering, Shahrood University of Technology, Shahrood, Iran

2 Department of Mechanical Engineering, University of California, Riverside, USA

3 School of Mechanical Engineering, University of Tehran, Tehran, Iran

4 Institute of Research and Development, Duy Tan University, Da Nang 550000, Vietnam

5 Faculty of Medicine, Duy Tan University, Da Nang 550000, Vietnam

and temperature of nanoparticle results in higher thermal conductivity of nanofluids. Utilization of hybrid nanofluids was suggested to improve the thermophysical properties of the nanofluid as well. Yildiz et al. [33] studied experimental and theoretical thermal conductivity model on thermal performance of a hybrid nanofluid. Al_2O_3–SiO_2/water hybrid nanofluid was used in their study. It was revealed that the use of hybrid nanoparticles can lead to the same heat transfer rate at lower particle volume fractions. In an experimental study by Shamaei et al. [34], it was shown that the increment in temperature and solid phase fraction of nanofluid can considerably increase its thermal conductivity. Different volume fractions and temperatures of double-walled carbon nanotubes (DWCNTs) suspended in ethylene glycol (EG) were considered. Cacua et al. [35] studied thermal conductivity of TiO_2/water nanofluid experimentally. During measurements of thermal conductivity, agitation of nanofluid was investigated, and it was shown that this can have considerable impact on the results since a great amount of nanoparticles can adhere to experimental apparatus. In addition, it was shown that thermal conductivity of the nanofluid increases markedly as the temperature rises.

The use of intelligence methods in determining thermal conductivity of nanofluids has become prevalent in recent years [36–39]. Artificial neural network (ANN) and support vector machine (SVM) are two common methods for modeling engineering problems [40]. Thermal conductivity of a nanofluid is dependent to various parameters like concentration and dimensions of nanoparticles as well as its temperature [41]. Group method of data handling (GMDH) and multilayer perceptron ANNs are broadly applied for estimating and forecasting the properties of nanofluids [41, 42]. In a study by Komeilibirjandi et al. [43], mathematical correlation and GMDH were investigated to predict nanofluids' thermal conductivity which had CuO nanoparticles. It was shown that the R-squared and the average absolute relative deviation for the artificial neural network method are more appropriate for prediction of thermal conductivity of nanofluids with CuO nanoparticles. Vafaei et al. [44] conducted an investigation of thermal conductivity of MgO-MWCNTs/EG hybrid nanofluid. Initially, thirty-six data set from experimental tests was considered. The temperature of the hybrid nanofluid was in the range of 25–50 °C, and six different nanoparticle volume fractions from 0.05 to 0.6% were considered. They studied four various artificial neural networks from 6 to 12 neurons in hidden layer. The results showed that the model of 12 neurons in hidden layer has the most favorable result with the maximum derivation of 0.8%. Different factors including the training algorithm of ANNs, their type and number of hidden neurons influence the reliability of the proposed models. Depending on the nature of the problem, these parameters can be obtained.

One of the nanoparticles which is widely employed in heat transfer fluids is silica (SiO_2). Nanofluids with SiO_2 are employed in different thermal devices such as solar collectors, heat exchangers and heat pipes. Favorable stability of these particles in different base fluids is one of its main advantages. In this study, thermal conductivity of nanofluids with SiO_2 particles is modeled by employing different ANN-based approaches. The selected methods for the modeling are GMDH and multilayer perceptron with two different training algorithms. The most important novelties of the present research are consideration of various base fluids and effect of size on the output of the model. Moreover, the performance of different ANN-based approaches is compared and investigated in terms of MSE and R-squared values. Finally, a correlation, based on GMDH, is proposed to determine the thermal conductivity of the considered nanofluids.

Methods

In this study, GMDH in addition to a conventional type of ANN with two training algorithms is applied for modeling the thermal conductivity of nanofluids with SiO_2 nanoparticles. These algorithms are selected for modeling since they have shown reliable outputs in several researches in this field. Mathematically, GMDH algorithm is based on the Volterra functional series in the form of bivariate quadratic polynomial as represented in Eq. (1) [45, 46].

$$y_i = f(x_i, x_j) = a_0 + a_1 x_i + a_2 x_j + a_3 x_i x_j + a_4 x_i^2 + a_5 x_j^2 \quad (1)$$

In this equation, the Volterra series is changed into a set of chain recursive equations; therefore, the Volterra series is regenerated by the algebraic repositioning of each of the recursive equations. Complex systems that include m input and an output variable can be decomposed to $c_m{}^2 = \frac{m(m-1)}{2}$ simple partial system with two inputs and one output. However, all the outputs are considered the same and equal to that of the complex system. To combine two partial systems into a single system and to form a new system that has variables from both former systems, it is sufficient to remodel the output of models with n inputs. GMDH algorithm performs modeling by applying two rules. The first one is to obtain a model in which almost all the variables of the system are represented. The second requirement is to obtain a model whose output error is lower than that of the other models that are calculated in the previous steps.

GMDH neural network is a self-organizing and one-directional network that has different layers in which each layer has several neurons. The neurons' structures are similar. Weights (w) are set in each neurons as specific and constant values on the basis of singular value decomposition (SVD)

and solving normal equation (SNE) techniques. The prominent feature seen in this type of network is that the neurons of the previous layer (m) are responsible for generation of c_m^2 new neurons. Among the generated neurons, some of them must be eliminated to prevent divergence of the network. These neurons are called dead neurons. This algorithm is described in more details in Refs. [47, 48].

In addition to GMDH multilayer perceptron (MLP), ANN is applied for modeling. The procedure of this algorithm has been explained in details in several articles [41, 42]. Various factors such as number of hidden layers and neurons in addition to the utilized training function affect the performance of these models. In the current study, two training algorithms including Levenberg–Marquardt and scaled conjugate gradient are used. Since the problem is not very complex, just one hidden layer is applied in the models. Different numbers of neurons from 3 to 10 are tested to determine the best one on the basis of mean square error (MSE) value. The appropriateness of the models and their accuracy are assessed on the basis of R-squared and MSE which are defined as [43]:

$$R^2 = 1 - \frac{\sum_{i=1}^{i=n} \left(y_i^{\text{experimental}} - y_i^{\text{predicted}}\right)^2}{\sum_{i=1}^{i=n} \left(y_i^{\text{experimental}} - \overline{y^{\text{experimental}}}\right)^2}$$

$$MSE = \frac{1}{n} \sum_{i=1}^{i=n} \left(y_i^{\text{experimental}} - y_i^{\text{predicted}}\right)^2.$$

Results and discussion

As indicated in the previous section, GMDH is one of the methods employed for thermal conductivity modeling. The data for modeling are obtained from various experimental studies which have investigated the thermal conductivity of nanofluids with silica particles and different base fluids such as water, ethylene glycol, glycerol and mixture of water and ethylene glycol [49–51]. The ranges of variables are shown in Table 1. For this method, the data sets were divided into two groups known as test and training. Here, 30% of data

Table 1 Variable ranges in the considered experimental studies

Variable	Range
Temperature/°C	25–60
Volume fraction of particles/%	0.1–3
Size of particles/nm	21–45
Base fluids	Water, ethylene glycol, glycerol and mixture of water and ethylene glycol

sets were randomly utilized for testing the trained networks. The obtained function for the thermal conductivity on the basis of the considered inputs is provided in Appendix, where x_1, x_2, x_3 and x_4 are base fluid thermal conductivity (W m^{-1} K^{-1}) at 25 °C, mean size of particles (nm), volume fraction of silica nanoparticles in base fluid (%) and temperature (°C), respectively. In Fig. 1, the values of thermal conductivity in actual condition (measured in experimental studies) are compared with outputs of the applied model. The value of R^2 for the case of applying GMDH is 0.9997.

The value of R^2 must be between 0 and 1. Closer values of R^2 to the unity demonstrate higher model reliability and lower differences between the actual values and the quantities obtained by the regression. In addition to this parameter, using relative error can be useful to assess the precision of the model. The maximum absolute value of this factor for the model proposed by using GMDH is approximately 1.75%, as shown in Fig. 2.

Similar to numerical and computational approaches [52–54], different parameters influence the output of model. Training algorithm is one the most important ones. Various training algorithms have been employed in multilayer perceptron ANNs. In this study, scaled conjugate gradient (SCG) and Levenberg–Marquardt (LM) have been tested. In addition to the training algorithm, ANN structure such as number of neurons influences the model performance. In this study, according to the complexity degree of the problem, one hidden layer is considered. Furthermore, different numbers of neurons in range of 3 and 10 were tested to find the most accurate one. The criterion used for comparing the models is MSE value. In Table 2, MSE values for different
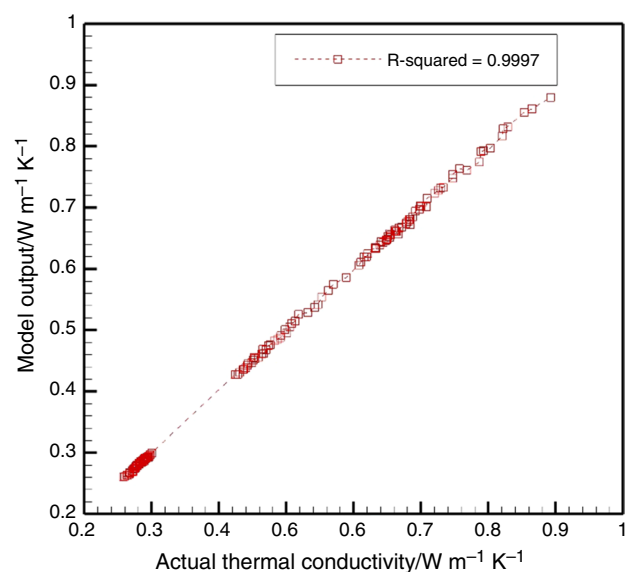

Fig. 1 Comparison of the model outputs and measured values for GMDH-based model
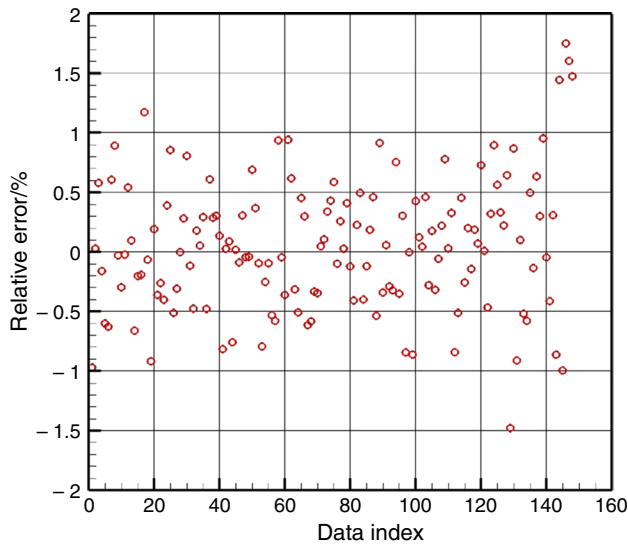
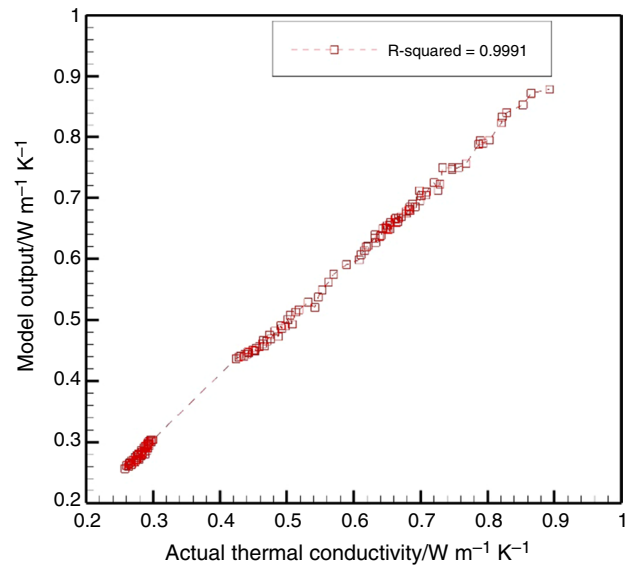**Fig. 2** Relative error of the predicted data for GMDH-based model

Fig. 3 Comparison of the model outputs and measured values for SCG-based model

Table 2 MSE values for different numbers of neurons for SCG-based model

Number of neurons in hidden layer	MSE
3	0.001862
4	0.000212
5	0.00059
6	0.000274
7	0.000576
8	**0.000032**
9	0.000295
10	0.000237

Fig. 4 Relative error of the predicted data for SCG-based model

numbers of neurons for the case of using SCG algorithm are represented. The minimum value of MSE, indicating the highest reliability, is obtained for 8 neurons in the hidden layer.

Since using 8 neurons results in the most favorable forecast, the outputs of the model are compared for this case. As illustrated in Fig. 3, R^2 is equal to 0.9991. Similar to GMDH-based model, the model is reliable based on its R^2 value since it is very close to 1. The relative error of the forecasted values is represented in Fig. 4. In the case of using multilayer perceptron with SCG training algorithm, the highest absolute relative error is approximately 4%.

Similar to the case of using SCG training algorithm, various numbers of hidden neurons are checked for LM algorithm. In Table 3, MSE values for different numbers of neurons are represented. In the case of employing LM for network training, the minimum value of MSE is obtained by applying 9 neurons in the hidden layer which is equal to 0.0000078. In comparison with the cases of utilizing SCG
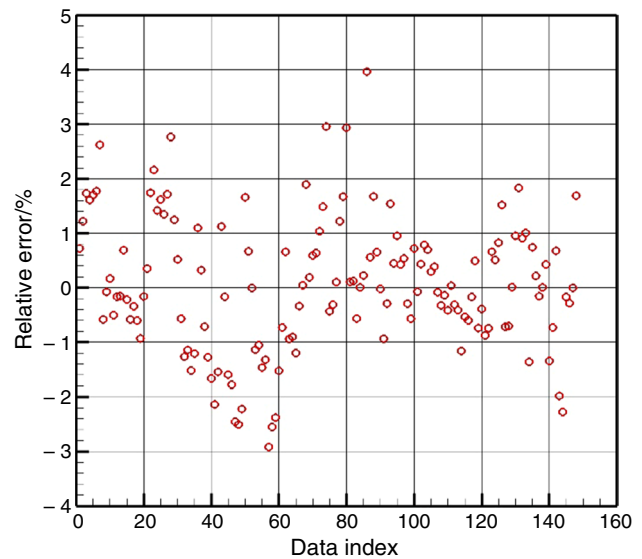
algorithm, MSE values of LM algorithms are lower which reveals more accurate performance of LM in training the network.

In Fig. 5, the determined data by LM method are compared with the measured thermal conductivities in the previous experimental studies. As shown in this figure, R^2 is 0.9998, which is very close to 1. In Fig. 6, relative error of the model that used LM algorithm for training is shown. In this condition, the maximum absolute relative error is

Table 3 MSE values for different numbers of neurons for LM-based model

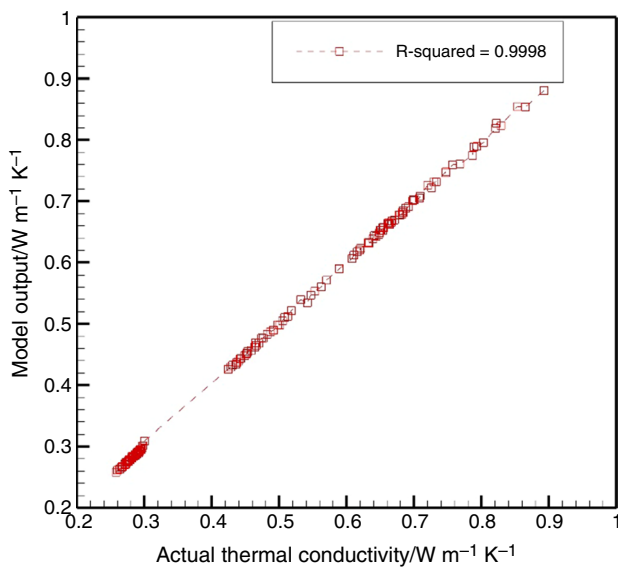| Number of neurons in hidden layer	MSE
3	0.000044
4	0.000021
5	0.0000085
6	0.000015
7	0.0000087
8	0.000014
9	**0.0000078**
10	0.000011

Fig. 7 MSE values of different approaches

Fig. 5 Comparison of the model outputs and measured values for LM-based model
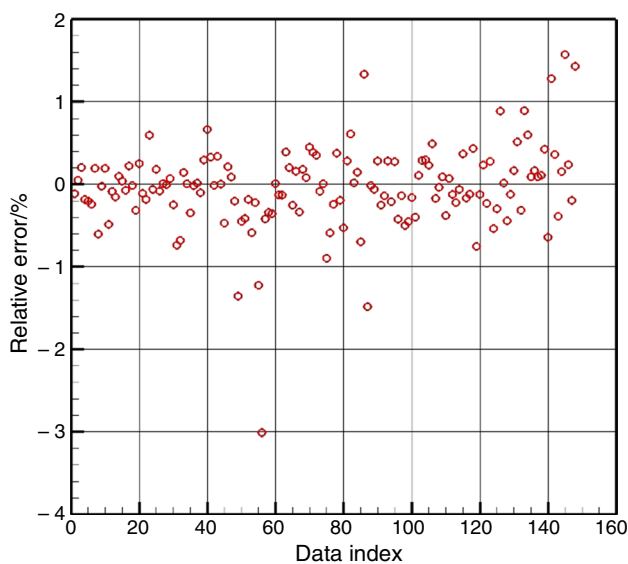
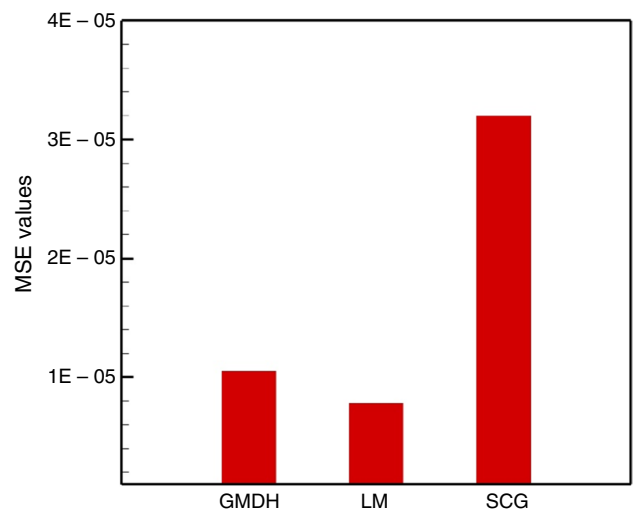**Fig. 6** Relative error of the predicted data for LM-based model

approximately 3%, which is higher than the corresponding value of the GMDH-based model.

In Fig. 7, MSE values of the different models are represented. As represented in this figure, the highest value of MSE belongs to the multilayer perceptron ANN with SCG training algorithm. Moreover, it can be noticed that using LM algorithm for training leads to the lowest MSE quantity. Despite the higher absolute relative error of the model in the case of using LM training algorithm compared with the GMDH approach, its MSE value is lower. This is due to lower deviation in the majority of predicted values in the case of applying LM.

Conclusions

Nanofluids containing silica particles are employable in thermal engineering since they have acceptable stability and favorable thermal properties. In the current article, MLP and GMDH neural networks are applied for thermal conductivity modeling. For the cases of applying MLP, two training algorithms including Levenberg–Marquardt and scaled conjugate gradient are evaluated. The main findings of the current study are summarized as follows:

- All of the trained ANNs are able to properly model thermal conductivity of the nanofluids.
- The accuracy of the proposed models is dependent on the training algorithm, utilized approach as well as network structure.
- The minimum value of MSE, which is approximately 0.0000078, is observed in case of applying ANN with Levenberg–Marquardt training algorithm.

- The values of R^2 in the cases of applying LM, SCG and GMDH are 0.9998, 0.9991 and 0.9997, respectively.
- Using 8 and 9 neurons in the hidden layer of trained networks with SCG and LM, respectively, results in obtaining the most accurate models.
- In all of the cases, the maximum relative deviations of the models does not exceed 4%, which reveals their acceptable reliability.

Appendix

$$Thermal\ conductivity = 0.00126014 - N46 * N2 * 97.3843$$
$$+ N46^2 * 48.6909 + N2 * 0.993462$$
$$+ N2^2 * 48.699$$

where

$$N2 = 9.37646 * 10^{-5} - N363 * 0.0335857 + N3 * 1.03339$$

$$N3 = -0.000874636 + N221 * 0.122798 + N221 * N4$$
$$* 11.3205 - N221^2 * 5.74673 + N4$$
$$* 0.882377 - N4^2 * 5.57863$$

$$N4 = -0.00215872 - N23 * 1.62829 - N23 * N7$$
$$* 2.48184 + N23^2 * 2.47217 + N7 * 2.63815$$

$$N7 = 0.000763705 + N230 * 0.304117$$
$$+ N230 * N13 * 6.8786 - N230^2 * 3.84272$$
$$+ N13 * 0.693187 - N13^2 * 3.03338$$

$$N13 = -2.22059 * 10^{-5} + N19 * 0.521767 + N23 * 0.478278$$

$$N19 = 0.00745006 - N406 * 0.325665$$
$$- N406 * N44 * 2.88803 + N406^2 * 1.75851$$
$$+ N44 * 1.29031 + N44^2 * 1.16405$$

$$N44 = -0.00373522 + N90 * 2.62726 + N90 * N111 * 81.2924$$
$$- N90^2 * 42.2947 - N111 * 1.61017 - N111^2 * 39.0116$$

$$N90 = 0.00439835 + N140 * N152 * 52.0459 - N140^2$$
$$* 25.4458 + N152 * 0.985753 - N152^2 * 26.586$$

$$N152 = 0.00164091 + N260 * 4.11528$$
$$+ N260 * N267 * 135.676 - N260^2$$
$$* 69.9834 - N267 * 3.11957 - N267^2 * 65.6878$$

$$N267 = -0.00647904 + N358 * 1.04195 - N358 * N568$$
$$* 6.13814 + N358^2 * 3.00401 + N568^2 * 3.0572$$

$$N568 = -3.84502 * 10^{-11} + N576$$

$$N140 = 0.0808505 - x_2 * 0.00549205 - x_2 * N301 * 0.0550408$$
$$+ x_2^2 * 0.000522728 + N301 * 0.968932 + N301^2 * 1.74424$$

$$N301 = -0.0144666 - N389 * 0.282082 + N389 * N504$$
$$* 1.90272 + N504 * 1.35027 - N504^2 * 1.97036$$

$$N389 = 0.14449 - x_4 * 0.00484756$$
$$+ x_4 * N505 * 0.0108732 + x_4^2 * 1.97213 * 10^{-5}$$
$$+ N505 * 0.654134 - N505^2 * 0.101332$$

$$N505 = -0.0488979 + \sqrt[3]{x_1} * \sqrt[3]{x_3} * 0.599567 + \sqrt[3]{x_1}^2$$
$$* 0.963904 - \sqrt[3]{x_3} * 0.580766 + \sqrt[3]{x_3}^2 * 0.121747$$

$$N406 = -0.0120488 - N483 * 56.7433 - N483$$
$$* N485 * 37520.8 + N483^2 * 18822.1 + N485$$
$$* 57.7807 + N485^2 * 18698.6$$

$$N485 = 0.0771466 + N510 * 0.61926 + N510 * N522$$
$$* 6.46372 - N510^2 * 3.19209 - N522^2 * 2.84671$$

$$N522 = -0.493982 - x_4 * 0.0135231 + x_4 *$$
$$\sqrt[3]{x_1} * 0.0212663 + \sqrt[3]{x_1} * 1.19902$$

$$N510 = -11.2593 + \sqrt[3]{x_2} * 7.12025 + \sqrt[3]{x_2}$$
$$* \sqrt[3]{x_3} * 0.111236$$
$$- \sqrt[3]{x_2}^2 * 1.06188 - \sqrt[3]{x_3} * 0.44152 + \sqrt[3]{x_3}^2 * 0.106266$$

$$N483 = 0.07833 + N512 * 0.612841 + N512 * N520$$
$$* 6.5401 - N512^2 * 3.22536 - N520^2 * 2.88274$$

$$N230 = -0.0006912 + N271 * 0.322697 + N271$$
$$* N340 * 0.705158 + N340 * 0.67916$$
$$- N340^2 * 0.705715$$

$$N340 = -0.110704 + N456 * 1.54893 - N456$$
$$* N571 * 5.64152 + N456^2 * 2.71745$$
$$+ N571^2 * 2.33681$$

$$N456 = 0.0665178 + N508 * 0.546738 + N508$$
$$* N516 * 6.96973 - N508^2 * 3.38871$$
$$+ N516 * 0.116385 - N516^2 * 3.19363$$

$$N271 = -0.00622633 + N353 * 1.04014 - N353 * N569$$
$$* 6.01031 + N353^2 * 2.93825 + N569^2 * 2.99795$$

$$N569 = -2.67753 * 10^{-11} + N575$$

$$N353 = 0.192405 - \sqrt[3]{x_3} * 0.302692 + \sqrt[3]{x_3}$$
$$* N516 * 0.317988 + \sqrt[3]{x_3}^2$$
$$* 0.123219 + N516 * 0.5975 + N516^2 * 0.0640845$$

$$N516 = -1.69737 + x_2 * 0.126947 + x_2$$
$$* x_4 * 0.000155269 - x_2^2 * 0.00175107$$
$$- x_4^2 * 2.86687 * 10^{-5}$$

$$N23 = 0.00447349 - N153 * N50 * 78.5724$$
$$+ N153^2 * 38.8351 + N50 * 0.977106$$
$$+ N50^2 * 39.7578$$

$$N50 = -0.00391508 + N84 * 1.99388 + N84$$
$$* N111 * 50.3034 - N84^2 * 26.4171 - N111$$
$$* 0.97457 - N111^2 * 23.9045$$

$$N111 = 0.00345229 + N384 * 0.521188 + N384$$
$$* N147 * 29.5477 - N384^2 * 15.4699 + N147$$
$$* 0.481536 - N147^2 * 14.0842$$

$$N384 = 0.20894 - \sqrt[3]{x_3} * 0.323349 + \sqrt[3]{x_3} * N520$$
$$* 0.31765 + \sqrt[3]{x_3}^2 * 0.13443 + N520 * 0.562513$$
$$+ N520^2 * 0.0980371$$

$$N84 = 0.000661737 + N143 * N153 * 69.385$$
$$- N143^2 * 34.1426 + N153 * 1.00566 - N153^2 * 35.2489$$

$$N153 = 0.0016409 + N260 * 4.11528 + N260 * N266$$
$$* 135.675 - N260^2 * 69.9831 - N266$$
$$* 3.11957 - N266^2 * 65.6875$$

$$N266 = -0.00647904 - N576 * N358 * 6.13814 + N576^2$$
$$* 3.0572 + N358 * 1.04195 + N358^2 * 3.00401$$

$$N576 = 6.28532 + x_1 * 9.35319 + x1$$
$$* \sqrt[3]{x_1} * 21.8155 - x_1^2 * 18.2776$$
$$- \sqrt[3]{x_1} * 11.9925 - \sqrt[3]{x_1}^2 * 7.78641$$

$$N221 = 3.45931 * 10^{-5} + N315 * 1.98289 + N315$$
$$* N363 * 9.78517 - N315^2 * 5.79152 - N363$$
$$* 0.98315 - N363^2 * 3.98824$$

$$N315 = -0.0353646 - N417 * 0.312089 - N417$$
$$* N504 * 6.73671 + N417^2$$
$$* 4.34277 + N504 * 1.47506 + N504^2 * 2.21611$$

$$N417 = 0.046616 - x_3 * 0.0227056 + x_3 * N523$$
$$* 0.0936959 + x_3^2 * 0.00319128 + N523$$
$$* 0.773515 + N523^2 * 0.0944211$$

$$N523 = 0.554784 - \sqrt[3]{x_1} * 0.446589 + \sqrt[3]{x_1}$$
$$* \sqrt[3]{x_4} * 0.735148 - \text{``} x4, cubert\text{''} * 0.468161$$

$$N363 = -0.113544 + N480 * 1.56256$$
$$- N480 * N571 * 4.71348 + N480^2$$
$$* 2.28464 + N571^2 * 1.82954$$

$$N571 = -1.05339 * 10^{-12} + N573$$

$$N573 = -0.619777 + x_2 * 0.0558848 + x_2$$
$$* \text{``} x1, cubert\text{''} * 0.0469653 - x_2^2 * 0.00128743$$
$$- \sqrt[3]{x_1} * 0.799765 + \sqrt[3]{x_1}^2 * 0.423977$$

$$N480 = 0.0793283 + N507 * 0.606649 + N507$$
$$* N520 * 6.5024 - N507^2 * 3.19284$$
$$- N520^2 * 2.87022$$

$$N520 = -0.0731976 + x_1 * 1.57015 + x_1$$
$$* x_4 * 0.01282 - x_1^2 * 0.98239$$
$$- x_4 * 0.00321404$$

$$N507 = -1.62014 + x_2 * 0.123157 + x_2$$
$$* x_3 * 0.00118382 - x_2^2 * 0.00162357$$

$$N46 = -0.00384249 + N87 * 2.23248 + N87 \\ * N112 * 15.7771 - N87^2 * 9.40143 \\ - N112 * 1.21432 - N112^2 * 6.39333$$

$$N112 = 0.00122818 + N402 * 0.497913 + N402 \\ * N147 * 23.2124 - N402^2 * 12.2215 \\ + N147 * 0.510862 - N147^2 * 11.0014$$

$$N147 = 0.0151096 - N517 * 0.733569 \\ + N517 * N248 * 1.09936 + N248 * 1.66087 \\ - N248^2 * 1.01956$$

$$N248 = -0.0312296 + x_1 * 0.215028 \\ - x_1 * N358 * 7.49913 + x_1^2 * 4.13888 \\ + N358 * 0.946609 + N358^2 * 3.23154$$

$$N402 = 0.0376697 - x_3 * 0.0223321 \\ + x_3 * N521 * 0.0940964 + x_3^2 * 0.00297722 \\ + N521 * 0.814425 + N521^2 * 0.053195$$

$$N521 = 0.180556 + x_1 * 0.565333 \\ + x_1 * \sqrt[3]{x_4} * 0.443784 - x_1^2 * 0.970109 \\ - \sqrt[3]{x_4} * 0.111981$$

$$N87 = 0.000661738 + N143 * N151 * 69.385 \\ - N143^2 * 34.1426 \\ + N151 * 1.00566 - N151^2 * 35.2488$$

$$N151 = 0.00164091 + N260 * 4.11528 \\ + N260 * N269 * 135.676 - N260^2 * 69.9834 \\ - N269 * 3.11957 - N269^2 * 65.6878$$

$$N269 = -0.00647904 - N575 * N358 * 6.13814 \\ + N575^2 * 3.0572 + N358 * 1.04195 \\ + N358^2 * 3.00401$$

$$N358 = 0.188766 - \sqrt[3]{x_3} * 0.299711 \\ + \sqrt[3]{x_3} * N519 * 0.317394 + \sqrt[3]{x_3}^2 * 0.121656 \\ + N519 * 0.608858 + N519^2 * 0.0534157$$

$$N519 = -11.1969 + \sqrt[3]{x_2} * 7.37547 \\ + \sqrt[3]{x_2} * \sqrt[3]{x_4} * 0.172616 - \sqrt[3]{x_2}^2 * 1.17692 \\ - \sqrt[3]{x_4} * 0.451075$$

$$N575 = -4.05032 - \sqrt[3]{x_1} * 3.8942 - \sqrt[3]{x_1} * \sqrt[3]{x_2} * 2.24393 \\ + \sqrt[3]{x_1}^2 * 8.41247 + \sqrt[3]{x_2} * 3.32065 - \sqrt[3]{x_2}^2 * 0.239694$$

$$N260 = -0.0159074 - x_1 * N341 * 7.38292 \\ + x_1^2 * 4.28392 + N341 * 1.07114 \\ + N341^2 * 3.08084$$

$$N341 = 0.191389 - \sqrt[3]{x_3} * 0.304664 \\ + \sqrt[3]{x_3} * N517 * 0.320767 + \sqrt[3]{x_3}^2 * 0.123665 \\ + N517 * 0.606339 + N517^2 * 0.0525463$$

$$N517 = -12.2238 - x_4 * 0.0130871 \\ + x_4 * \sqrt[3]{x_2} * 0.00500479 \\ + \sqrt[3]{x_2} * 7.77345 - \sqrt[3]{x_2}^2 * 1.17885$$

$$N143 = 2.65296 - \sqrt[3]{x_2} * 2.27093 \\ - \sqrt[3]{x_2} * N285 * 1.69357 \\ + \sqrt[3]{x_2}^2 * 0.497524 + N285 * 4.57061 + N285^2 * 1.71161$$

$$N285 = -0.0129764 - N383 * 0.270567 \\ + N383 * N504 * 1.89115 \\ + N504 * 1.33173 - N504^2 * 1.95175$$

$$N504 = -0.438416 + x_2 * 0.0407094 \\ - x_2 * N512 * 0.0702555 + N512 * 0.204885 \\ + N512^2 * 2.79313$$

$$N512 = -1.50849 + x_2 * 0.119589 \\ + x_2 * \sqrt[3]{x_3} * 0.0034988 - x_2^2 * 0.00160038 \\ - \sqrt[3]{x_3} * 0.201899 + \sqrt[3]{x_3}^2 * 0.105077$$

$$N383 = 1.00566 - \sqrt[3]{x_4} * 0.494159 \\ + \sqrt[3]{x_4} * N508 * 0.391485 + \sqrt[3]{x_4}^2 * 0.0549278 \\ - N508 * 0.153024 - N508^2 * 0.189057$$

$$N508 = -0.240191 - x_3 * 0.10489 \\ + x_3 * \sqrt[3]{x_1} * 0.187864 + \sqrt[3]{x_1}^2 * 1.2194.$$

References

1. Gandomkar A, Kalan K, Vandadi M, Shafii MB, Saidi MH. Investigation and visualization of surfactant effect on flow pattern and

performance of pulsating heat pipe. J Therm Anal Calorim. 2019. https://doi.org/10.1007/s10973-019-08649-z.

2. Alizadeh H, Ghasempour R, Shafii MB, Ahmadi MH, Yan W-M, Nazari MA. Numerical simulation of PV cooling by using single turn pulsating heat pipe. Int J Heat Mass Transf. 2018;127:203–8.

3. Toghyani S, Afshari E, Baniasadi E, Shadloo MS. Energy and exergy analyses of a nanofluid based solar cooling and hydrogen production combined system. Renew Energy. 2019;141:1013–25.

4. Karimipour A, Bagherzadeh SA, Goodarzi M, Alnaqi AA, Bahiraei M, Safaei MR, et al. Synthesized CuFe$_2$O$_4$/SiO$_2$ nanocomposites added to water/EG: evaluation of the thermophysical properties beside sensitivity analysis & EANN. Int J Heat Mass Transf. 2018;127:1169–79.

5. Sørensen DN, Voigt LK. Modelling flow and heat transfer around a seated human body by computational fluid dynamics. Build Environ. 2003;38:753–62.

6. De Dear RJ, Arens E, Hui Z, Oguro M. Convective and radiative heat transfer coefficients for individual human body segments. Int J Biometeorol. 1997;40:141–56.

7. Ghanami S, Farhadi M. Heat transfer enhancement in a single-pipe heat exchanger with fluidic oscillators. J Therm Anal Calorim. 2019;1–13.

8. Arasteh H, Mashayekhi R, Ghaneifar M, Toghraie D, Afrand M. Heat transfer enhancement in a counter-flow sinusoidal parallel-plate heat exchanger partially filled with porous media using metal foam in the channels' divergent sections. J Therm Anal Calorim. 2019;1–17.

9. Hasanpour B, Irandoost MS, Hassani M, Kouhikamali R. Numerical investigation of saturated upward flow boiling of water in a vertical tube using VOF model: effect of different boundary conditions. Heat Mass Transf Stoffuebertragung. 2018;54:1925–36.

10. Gholamalipour P, Siavashi M, Doranehgard MH. Eccentricity effects of heat source inside a porous annulus on the natural convection heat transfer and entropy generation of Cu-water nanofluid. Int Commun Heat Mass Transf. 2019;109:104367.

11. Ramezanizadeh M, Alhuyi Nazari M, Hossein Ahmadi M, Chen L. A review on the approaches applied for cooling fuel cells. Int J Heat Mass Transf. 2019;139:517–25.

12. Abdollahzadeh Jamalabadi M, Ghasemi M, Alamian R, Wongwises S, Afrand M, Shadloo M. Modeling of subcooled flow boiling with nanoparticles under the influence of a magnetic field. Symmetry. 2019;11:1275. https://www.mdpi.com/2073-8994/11/10/1275

13. Choi SUS, Eastman JA. Enhancing thermal conductivity of fluids with nanoparticles. ASME international mechanical engineering congress & exposition. American Society of Mechanical Engineers, San Francisco, 1995.

14. Gandomkar A, Saidi MH, Shafii MB, Vandadi M, Kalan K. Visualization and comparative investigations of pulsating ferro-fluid heat pipe. Appl Therm Eng. 2017;116:56–655.

15. Heydarian R, Shafii MB, Rezaee Shirin-Abadi A, Ghasempour R, Alhuyi Nazari M. Experimental investigation of paraffin nano-encapsulated phase change material on heat transfer enhancement of pulsating heat pipe. J Therm Anal Calorim. 2019;137:1603–13. https://doi.org/10.1007/s10973-019-08062-6.

16. Ajeel RK, Salim WSI, Sopian K, Yusoff MZ, Hasnan K, Ibrahim A, et al. Turbulent convective heat transfer of silica oxide nanofluid through corrugated channels: An experimental and numerical study. Int J Heat Mass Transf. 2019;145:118806.

17. Qi C, Luo T, Liu M, Fan F, Yan Y. Experimental study on the flow and heat transfer characteristics of nanofluids in double-tube heat exchangers based on thermal efficiency assessment. Energy Convers Manag. 2019;197:111877.

18. Safaei MR, Togun H, Vafai K, Kazi SN, Badarudin A. Investigation of heat transfer enhancement in a forward-facing contracting

19. channel using FMWCNT nanofluids. Numer Heat Transf A Appl. 2014;66:1321–40.

19. Byrne MD, Hart RA, Da Silva AK. Experimental thermal-hydraulic evaluation of CuO nanofluids in microchannels at various concentrations with and without suspension enhancers. Int J Heat Mass Transf. 2012;55:2684–91.

20. Kalteh M, Abbassi A, Saffar-Avval M, Frijns A, Darhuber A, Harting J. Experimental and numerical investigation of nanofluid forced convection inside a wide microchannel heat sink. Appl Therm Eng. 2012;36:260–8.

21. Behnampour A, Akbari OA, Safaei MR, Ghavami M, Marzban A, Sheikh Shabani GA, et al. Analysis of heat transfer and nanofluid fluid flow in microchannels with trapezoidal, rectangular and triangular shaped ribs. Phys E Low-Dimens Syst Nanostruct. 2017;91:15–311.

22. Irandoost Shahrestani M, Maleki A, Safdari Shadloo M, Tlili I. Numerical investigation of forced convective heat transfer and performance evaluation criterion of Al$_2$O$_3$/water nanofluid flow inside an axisymmetric microchannel. Symmetry 2020;12:120. https://www.mdpi.com/2073-8994/12/1/120

23. Kalteh M. Investigating the effect of various nanoparticle and base liquid types on the nanofluids heat and fluid flow in a microchannel. Appl Math Model. 2013;37:8600–9.

24. Mohammed HA, Gunnasegaran P, Shuaib NH. The impact of various nanofluid types on triangular microchannels heat sink cooling performance. Int Commun Heat Mass Transf. 2011;38:767–73.

25. Bayat J, Nikseresht AH. Investigation of the different base fluid effects on the nanofluids heat transfer and pressure drop. Heat Mass Transf Stoffuebertragung. 2011;47:1089–99.

26. Siavashi M, Karimi K, Xiong Q, Doranehgard MH. Numerical analysis of mixed convection of two-phase non-Newtonian nanofluid flow inside a partially porous square enclosure with a rotating cylinder. J Therm Anal Calorim. 2019;137:267–87.

27. Joibary SMM, Siavashi M. Effect of Reynolds asymmetry and use of porous media in the counterflow double-pipe heat exchanger for passive heat transfer enhancement. J Therm Anal Calorim. 2019;1–15.

28. Siavashi M, Talesh Bahrami HR, Aminian E, Saffari H. Numerical analysis on forced convection enhancement in an annulus using porous ribs and nanoparticle addition to base fluid. J Cent South Univ. 2019;26:1089–98.

29. Bagherzadeh SA, Sulgani MT, Nikkhah V, Bahrami M, Karimipour A, Jiang Y. Minimize pressure drop and maximize heat transfer coefficient by the new proposed multi-objective optimization/statistical model composed of "ANN + Genetic Algorithm" based on empirical data of CuO/paraffin nanofluid in a pipe. Phys A Stat Mech Appl. 2019;527:121056.

30. Ramezanizadeh M, Ahmadi MA, Ahmadi MH, Alhuyi Nazari M. Rigorous smart model for predicting dynamic viscosity of Al$_2$O$_3$/water nanofluid. J Therm Anal Calorim. 2018. https://doi.org/10.1007/s10973-018-7916-1.

31. Wang N, Maleki A, Alhuyi Nazari M, Tlili I, Safdari Shadloo MS. Thermal conductivity modeling of nanofluids contain MgO particles by employing different approaches. Symmetry. 2020;12(2):206.

32. Ahmadi MH, Mirlohi A, Alhuyi Nazari M, Ghasempour R. A review of thermal conductivity of various nanofluids. J Mol Liq. 2018;265:181–8.

33. Yıldız Ç, Arıcı M, Karabay H. Comparison of a theoretical and experimental thermal conductivity model on the heat transfer performance of Al$_2$O$_3$–SiO$_2$/water hybrid-nanofluid. Int J Heat Mass Transf. 2019;140:598–605.

34. Shamaeil M, Firouzi M, Fakhar A. The effects of temperature and volume fraction on the thermal conductivity of functionalized DWCNTs/ethylene glycol nanofluid. J Therm Anal Calorim. 2016;126:1455–62. https://doi.org/10.1007/s10973-016-5548-x.

35. Cacua K, Murshed SMS, Pabón E, Buitrago R. Dispersion and thermal conductivity of TiO$_2$/water nanofluid. J Therm Anal Calorim. 2019;1–6.

36. Ramezanizadeh M, Alhuyi NM. Modeling thermal conductivity of Ag/water nanofluid by applying a mathematical correlation and artificial neural network. Int J Low-Carbon Technol. 2019. https://doi.org/10.1093/ijlct/ctz030/5552090.

37. Hemmat EM. Designing an artificial neural network using radial basis function (RBF-ANN) to model thermal conductivity of ethylene glycol–water-based TiO2nanofluids. J Therm Anal Calorim. 2017;127:2125–31.

38. Hemmat Esfe M, Naderi A, Akbari M, Afrand M, Karimipour A. Evaluation of thermal conductivity of COOH-functionalized MWCNTs/water via temperature and solid volume fraction by using experimental data and ANN methods. J Therm Anal Calorim. 2015;121:1273–8.

39. Hemmat Esfe M, Wongwises S, Naderi A, Asadi A, Safaei MR, Rostamian H, et al. Thermal conductivity of Cu/TiO$_2$–water/EG hybrid nanofluid: experimental data and modeling using artificial neural network and correlation. Int Commun Heat Mass Transf. 2015;66:100–4.

40. Nabipour N, Daneshfar R, Rezvanjou O, Mohammadi-Khanaposhtani M, Baghban A, Xiong Q, et al. Estimating biofuel density via a soft computing approach based on intermolecular interactions. Renew Energy. 2020;152:1086–98.

41. Ramezanizadeh M, Alhuyi Nazari M, Ahmadi MH, Lorenzini G, Pop I. A review on the applications of intelligence methods in predicting thermal conductivity of nanofluids. J Therm Anal Calorim. 2019. https://doi.org/10.1007/s10973-019-08154-3.

42. Ramezanizadeh M, Ahmadi MH, Nazari MA, Sadeghzadeh M, Chen L. A review on the utilized machine learning approaches for modeling the dynamic viscosity of nanofluids. Renew Sustain Energy Rev. 2019;114:109345.

43. Komeilibirjandi A, Raffiee AH, Maleki A, Alhuyi Nazari M, Safdari Shadloo M. Thermal conductivity prediction of nanofluids containing CuO nanoparticles by using correlation and artificial neural network. J Therm Anal Calorim. 2019. https://doi.org/10.1007/s10973-019-08838-w.

44. Vafaei M, Afrand M, Sina N, Kalbasi R, Sourani F, Teimouri H. Evaluation of thermal conductivity of MgO-MWCNTs/EG hybrid nanofluids based on experimental data by selecting optimal artificial neural networks. Phys E Low-Dimens Syst Nanostruct. 2017;85:90–6. https://doi.org/10.1016/j.physe.2016.08.020.

45. Pourkiaei SM, Ahmadi MH, Hasheminejad SM. Modeling and experimental verification of a 25W fabricated PEM fuel cell by parametric and GMDH-type neural network. Mech Ind. 2016;17:105. https://doi.org/10.1051/meca/2015050.

46. Kasaeian A, Ghalamchi M, Ahmadi MH, Ghalamchi M. GMDH algorithm for modeling the outlet temperatures of a solar chimney based on the ambient temperature. Mech Ind. 2017;18:216. https://doi.org/10.1051/meca/2016034.

47. Ahmadi MH, Sadeghzadeh M, Raffiee AH, Chau K. Applying GMDH neural network to estimate the thermal resistance and thermal conductivity of pulsating heat pipes. Eng Appl Comput Fluid Mech. 2019;13:327–36. https://doi.org/10.1080/19942060.2019.1582109.

48. Mohamadian F, Eftekhar L, Haghighi Bardineh Y. Applying GMDH artificial neural network to predict dynamic viscosity of an antimicrobial nanofluid. Mashhad Univ Med Sci Nanomed J. 2018;5:217–21. https://nmj.mums.ac.ir/article_11600.html

49. Akilu S, Baheta AT, Minea AA, Sharma KV. Rheology and thermal conductivity of non-porous silica (SiO$_2$) in viscous glycerol and ethylene glycol based nanofluids. Int Commun Heat Mass Transf. 2017;88:245–53.

50. Esfahani MA, Toghraie D. Experimental investigation for developing a new model for the thermal conductivity of silica/water-ethylene glycol (40%–60%) nanofluid at different temperatures and solid volume fractions. J Mol Liq. 2017;232:105–12.

51. Ranjbarzadeh R, Kazerouni AM, Bakhtiari R, Asadi A, Afrand M. An experimental study on stability and thermal conductivity of water/silica nanofluid: eco-friendly production of nanoparticles. J Clean Prod. 2018;206:1089–100.

52. Saffarian MR, Bahoosh R, Doranehgard MH. Entropy generation in the intake pipe of an internal combustion engine. Eur Phys J Plus. 2019;134(9):476.

53. Asadi A, Kadijani ON, Doranehgard MH, Bozorg MV, Xiong Q, Shadloo MS, et al. Numerical study on the application of biodiesel and bioethanol in a multiple injection diesel engine. Renew Energy. 2019;150:1019–29.

54. Bozorg MV, Doranehgard MH, Hong K, Xiong Q, Li LKB. A numerical study on discrete combustion of polydisperse magnesium aero-suspensions. Energy. 2020;194:116872.